Design of heart phantoms for ultrasound imaging of ventricular septal defects

Gerardo Tibamoso-Pedraza · Iñaki
Navarro · Patrice Dion · Marie-Josée
Raboisson · Chantale Lapierre ·
Joaquim Miró · Sylvie Ratté · Luc
Duong

Abstract Purpose: Ventricular Septal Defects (VSDs) are common congenital heart malformations. Echocardiography used during VSD hybrid cardiac procedures requires extensive training for image acquisition and interpretation. Cardiac surgery simulators with heart phantoms have shown usefulness for such training, but they are limited in visualization and characterization of complex VSD. This study explores a new method to build patient-specific heart phantoms with VSD, with proper tissue echogenicity for ultrasound imaging.

Methods: Heart phantoms were designed from preoperative imaging of three patients with complex VSDs. Each whole heart phantom, including atrial and ventricular septums, was obtained by manual segmentation and by surface reconstruction, then by molding and by casting in different materials. Heart phantoms in silicone and PolyVinyl Alcohol Cryogel (PVA-C) were considered and they were reconstructed in 3-D using 2-D freehand ultrasound imaging.

Results: An electromagnetic measurement system (EMS) was used to measure the mean VSD diameters from the heart phantoms. Errors were evaluated below 1.0 mm for mean VSD diameters between 6.2 and 7.5 mm.

Conclusion: Patient-specific heart phantoms promise for representing complex heart malformations such as VSDs. PVA-C showed better tissue echogenicity than silicone for VSDs visualization and characterization.

Keywords Ventricular septal defects · Heart phantoms · 3-D printing · Echocardiography

G. Tibamoso-Pedraza, P. Dion, S. Ratté, L. Duong
Interventional Imaging Lab, Department of software and IT engineering, École de technologie supérieure, 1100 Notre-Dame West, Montreal H3C 1K3, Canada
E-mail: gerardo.tibamoso-pedraza.1@etsmtl.net

I. Navarro, M.J. Raboisson, C. Lapierre, J. Miró
Cardiology, Department of Pediatrics, CHU Sainte-Justine, Montreal H3T 1C5, Canada

1 Introduction

Ventricular septal defects (VSDs) are common congenital heart malformations in newborns. VSDs leave holes in the ventricular septum that could cause pulmonary overflow and heart failure [1]. Complex VSDs are treated using a hybrid procedure, combining both cardiac surgery and cardiac catheterization, recommended when an open heart surgery is less feasible. The hybrid procedure is underpinned by echocardiography to guide an implant device to close the holes during beating heart [2].

The severity of VSDs depends on the size, shape, and location of the holes; characteristics generally identified by means of echocardiography[1]. Echocardiography is a complex image modality; hence, extensive training is required for an appropriate image acquisition and interpretation. Training with heart simulators could complement learning of echocardiography during hybrid procedures [3]; however, the cost and complexity of the simulators could hinder the possibility to include patient-specific heart models with complex VSDs.

Rapid prototyping has been used to build patient-specific heart models with complex VSDs [4]; however, commercial materials, such as plastics and resins, are still not appropriate to build models for ultrasound imaging. To overcome this limitation, casting has been used, which requires molds to reproduce heart models (phantoms) in a broader spectrum of materials. Indeed, water-based (PolyVinyl Alcohol Cryogel [PVA-C]) and no water-based (silicone and ballistic gel) materials have been tested using casting [5–7].

Morais et al. [5] proposed a method to build heart phantoms to represent the atriums and the inter-atrial septum. Laing et al. [6] proposed a method to build heart phantoms to represent an extensive atrioventricular region including the mitral valve. Alves et al. [7] proposed a method to build phantoms of the whole heart (atriums and ventricles) with the interest to evaluate its acoustic properties. For casting, Morais et al. [5] and Laing et al. [6] tested silicone and PVA-C, and Alves et al. [7] tested ballistic gel. Morais et al. [5] found similar behavior from both materials when they were scanned with ultrasound. Morais et al. [5] and Laing et al. [6] found that silicone has advantages over PVA-C considering processing complexities, production times, and preservation requirements. However, an appealing quality of PVA-C is its potential capacity to resemble mechanical properties of biological tissues given its high water content [5, 8–10]. Alves et al. [7] found a recipe with ballistic gel to mimic acoustic properties of biological tissues. Finally, from the ultrasound images reported by Morais et al. [5], Laing et al. [6], and Alves et al. [7] we observed similar attenuation patterns of the models made of silicone and ballistic gel.

The main goal of this study is to build heart phantoms of newborns with complex VSDs. The specific goals are to validate with two different materials (silicone and PVA-C), to evaluate measurements of the VSDs, and finally, to provide valuable insights on the design of heart phantoms for ultrasound imaging of VSDs.

2 Materials and Methods

From preoperative scans (computed tomography [CT] or cardiac magnetic resonance [CMR]), we designed heart phantoms of newborns with VSDs. The method is divided in three main steps: image segmentation, molding, and casting. For validation, we acquired 2-D ultrasound images from three heart phantoms, reconstructed a volume representation, and evaluated ventricular shapes and sizes of VSDs.

2.1 Dataset

Three retrospective cases of newborns with complex VSDs were collected from Sainte-Justine Hospital. The data included two CT and one CMR preoperative scans, with image resolution of 0.23 x 0.23 x 0.4 mm^3, 0.27 x 0.27 x 1.25 mm^3, and 0.63 x 0.63 x 5 mm^3, respectively. Before image segmentation, we redefined image's resolution of cases two and three to 0.27 x 0.27 x 0.27 mm^3, and 0.63 x 0.63 x 0.63 mm^3, respectively, using cubic interpolation. This step allowed us to segment regions with more detail and obtain smooth boundaries.

2.2 Cardiac Image Segmentation

We manually segmented images from the scans–guided by a cardiologist–to shape a 3-D region that includes left and right atriums, left and right ventricles, pulmonary artery, and aorta and filling spaces between them to obtain a solid body of the whole heart. From this region, we extracted boundaries of 3 mm thickness, and afterwards we segmented the septum's region to define the ventricular and atrial cavities. Then, we divided the remaining structure in two parts (atriums and ventricles), and added rims in their boundaries to facilitate their assembly after casting (Fig. 1). Finally, the segmented regions were modeled as polygonal meshes. For all these operations, we used 3D Slicer (www.slicer.org), which facilitates navigation in the 3-D data and the use of binary operations to refine and smooth the segmented regions.
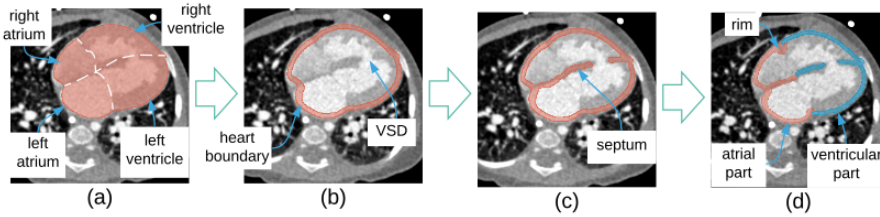

Fig. 1 Cardiac image segmentation. (a) Whole heart segmentation, (b) heart boundaries' extraction, (c) septum demarcation, and (d) separation of atrial and ventricular parts.

The polygonal meshes, which represent the whole heart (atriums and ventricles), were refined using Meshlab (www.meshlab.net). Basic boundary-preserving decimation and smoothing filters were applied to reduce the number of polygons while preserving anatomical details. These were the reference models for both the molds design (casting) and the comparison with the reconstructed models from the heart phantoms in the validation step.

2.3 Molding and Casting Heart Phantoms

We designed molds to reproduce the two parts of each heart phantom in two different materials: PVA-C and silicone. Afterwards, the parts were assembled to shape whole heart phantoms (Fig. 2).
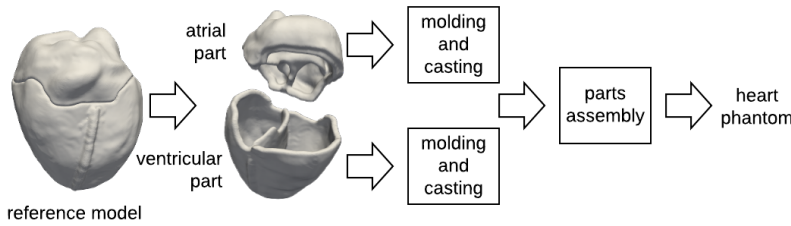

Fig. 2 Steps to build a heart phantom. Atrial and ventricular parts are reproduced individually, and they are assembled to shape a whole heart phantom.

2.3.1 Molding

The initial mold design was obtained by computing the Boolean difference between a solid block and each part of the models. We chose a cylindrical shape for the solid block, which is divided in two pieces for unmolding purposes. Then, two holes were added to the mold: one that connects with deep regions to pour the silicone or PVA-C for a bottom-up filling; the other connects with the regions at the top to allow the exit of air bubbles. Additional partitions to the mold were made to facilitate unmolding after casting. The mold's pieces were aligned with pin-hole pairs made in corresponding faces (Fig. 3). We used Autodesk Meshmixer for the mold design (www.meshmixer.com).

The mold's pieces were printed in 3-D with thermoplastic polymer (Materio3D PLA 3D850 1.75mm) by an Original Prusa i3 MKS (Prusa Research, Prague, Czech Republic) with the following settings: layer height=0.15 mm, infill=15%, support=none, and brim=off. The printed pieces were assembled and tied with plastic bands, and fissures between them were filled with a fine layer of commercial silicone to avoid leaking. However, before the assembly, we spread a fine layer of petroleum jelly (petrolatum 100%) to the opposite faces of the pieces that shape the VSDs, which aimed to inhibit the cure of
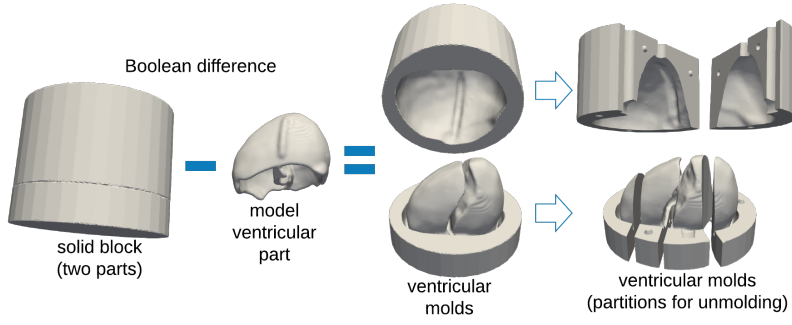
Fig. 3 Molds design. Boolean difference is the main operation, followed by partition of the molds to facilitate the unmolding after casting.

silicone or restrain the access of PVA-C in that region and assure the holes in the phantoms.

2.3.2 Casting with Silicone

We chose Smooth-On Ecoflex 00-30 (Smooth-On, PA, USA), platinum catalyzed silicone, which has shown good results modeling atrial cavities for ultrasound imaging [6]. We followed the manufacturer's instructions to prepare the silicone, namely mixing components A and B (equal proportions), and degassing the mix in a vacuum chamber (-30 inHg). We noticed that the time for mixing and degassing is short (5 min approx.), because the viscosity of the silicone increases quickly. Also for this reason, we prepared silicone for each mold individually. Immediately after its degassing, the silicone was poured into the molds and let to rest in it for 12 hours at room temperature before unmolding. After unmolding, the two parts of the phantom were assembled and glued together with a fine layer of a new preparation of the same silicone, and left them to rest for 12 more hours. For the assembly, the two parts were supported on the external section of the ventricular mold.

2.3.3 Casting with PVA-C

PVA hydrogel, which is the base for the PVA-C, was produced mixing PVA and distilled water in a proportion of 15 % and 85 % by weight, respectively. The PVA's properties that we used include 98-98.8 % hydrolyzed and M.W. approx. 50.000-85.000 (ACROS ORGANICS, Thermo Fisher Scientific, MA, USA, code: 183381000). The components were constantly mixed in an Erlenmeyer flask with a magnetic stir bar (180 rpm), over a heater plate that kept the mix at 80-90 °C, until the PVA was dissolved (2-3 h approx.). The level of the mix was supervised during all the mixing time, and distilled water was added when required. Thereafter, the resultant hydrogel was left at rest for 6h to reach room temperature and to release any remaining air bubbles.

Then, the PVA hydrogel was poured into the molds, let to rest for a couple of hours (allowing the exit of air bubbles), and exposed to three freeze-thaw cycles to form the PVA Cryogel (PVA-C). We used a commercial freezer, but we instrumented it to control the change of temperatures in a stair-wise manner. The instrumentation included a temperature sensor inside the freezer, a relay in one of the lines of the freezer power connector, and a Raspberry Pi that received the sensor information and controlled the relay.

Each freeze-thaw cycle began from room temperature (20 °C approx.) to -20 °C, with a freezing rate of -0.2 °C/min on average. Then, the temperature was held on -20 ± 2 °C for 6 h (control on-off between -18 and -22 °C). Afterwards, the temperature increased from -20 °C to 20 °C with a thawing rate of 0.06 °C/min on average (low thawing rates benefits the PVA-C formation [8]). After the three cycles, we unmolded and assembled the two parts that shape each heart phantom, using the external parts of the ventricular molds as support. In order to glue the parts firmly, three additional freeze-thaw cycles were required (cycles with the same properties as before), spreading a layer of the PVA hydrogel in the junctures just before the beginning of each cycle. Finally, the phantoms were kept under water and refrigerated (5 °C) for their preservation.

2.4 Validation

We acquired ultrasound (US) images from the heart phantoms to evaluate the shape of ventricular cavities and sizes of VSDs. To do this, we reconstructed 3-D models of the phantoms from their images. These models were compared with the respective models of reference. We used Dice similarity coefficient (DSC) to measure shape similarity between them, and estimated areas and diameters of VSDs.

The models' reconstruction involved 3-D reconstruction of the ultrasound images. For the latter, we recorded the position and orientation of the US probe together with the respective US images during the scanning of the ventricular region of each phantom that was full of and immersed in water. We obtained 3-D ultrasound reconstructions with 0.5 x 0.5 x 0.5 mm^3 resolution, using the volume reconstruction algorithm included in the PLUS toolkit library [11]. Then, we manually segmented the reconstructed images for the reconstruction of each model.

The images were acquired with a TOSHIBA PLT-704AT 7.5 MHz Linear array transducer (US probe), and the probe position and orientation–six degrees of freedom (6 DOF)–were recorded with an electromagnetic measurement system (EMS) (Aurora V2, NDI, Canada) (Fig. 4). The system was calibrated with the fCal algorithm included in the PLUS toolkit library. The accuracy of EMS measurements is evaluated at 0.48 mm RMS; the calibration error was less than 0.60 mm for each step of the algorithm. We relied on this acquisition system because of availability, accessibility, controlled environment, and acquisitions with a large field of view.
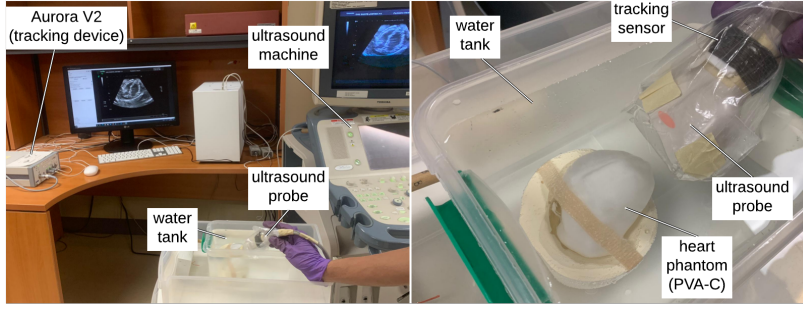
Fig. 4 3-D ultrasound reconstruction. (Left) Setup that includes ultrasound machine, electromagnetic tracking device (Aurora V2), desktop computer, and a water tank. (Right) A heart phantom in the water tank for ultrasound image acquisition.

Afterwards, the respective reconstructed and reference models were aligned with rigid transformations in two steps. The first step transformed one model towards the other aligning four corresponding points, which were defined manually over the two surfaces. The second step automatically refined the alignment of the models by an Iterative Closest Points algorithm (ICP). Finally, the models were transformed into image segmentation, and DSC was calculated. The tools for alignment and DSC calculation were found in 3D Slicer (slicerIGT and SegmentRegistration extensions).

On the other hand, sizes of the VSDs were estimated covering the area of the holes with triangular segments. For each hole, all triangular segments had a common vertex, the center of the hole, and the other vertices were regularly spaced along the hole's boundaries. From these partitions, area and size (diameters) of a VSD were estimated. The area was estimated adding up the areas of all the triangular segments; the diameters, adding up the magnitude of each pair of triangle's edges that touch the common vertex and are 180° apart, obtaining a list of values from where we calculated maximum, minimum, mean, and standard deviation.

3 Results

Four large VSDs were identified and represented accordingly in the reference heart models from the three retrospective cases (Fig. 5). VSDs diameters were between 4.8 mm and 8.8 mm (Table 1). Dimensions of the one, two, and three heart models were 80 x 65 x 55 mm^3, 70 x 60 x 45 mm^3, and 80 x 60 x 50 mm^3, respectively. Some images of the casting process are presented in Fig. 6. The reusable molds allowed us to reproduce similar phantoms made of silicone or PVA-C. Less than 100 ml of the silicone or PVA hydrogel was required to build a whole heart phantom.
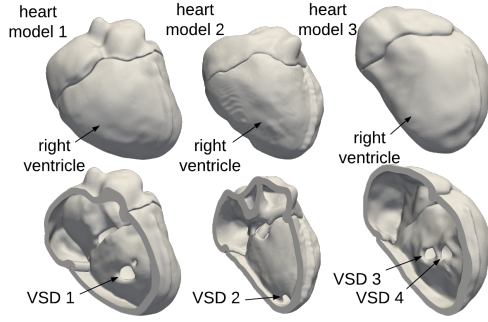
Fig. 5 Reference heart models. Upper row shows the assembled heart models; lower row shows the ventricular septums and VSDs of the models.
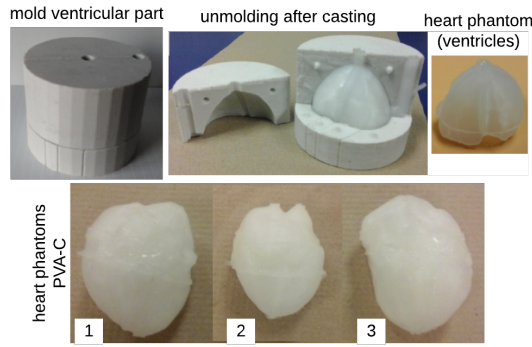

Fig. 6 Casting a heart phantom. Images of a mold, unmolding, and the final results to make heart phantoms.

3.1 Validation

We acquired ultrasound images from the phantoms made of silicone and also from those of PVA-C (Fig. 7). Boundaries of VSDs of the models made of silicone were not clear enough for image segmentation. In contrast, we observed better definition of VSDs in the images of the phantoms made of PVA-C. Hence, only reconstructions of the phantoms made of PVA-C were obtained; therefore, the following measurements are related to them.

Fig. 8 compares reference and reconstructed phantoms, where we can see shape similarities between ventricular regions. The DSC for each of the three heart phantoms was evaluated respectively at 0.71, 0.76, and 0.64. We estimated diameters and areas of the four large VSDs in the reference and reconstructed models of the three heart phantoms (Table 1 and Table 2). For all four VSDs, absolute value of errors in minimum (min.) and mean diameters were lower than 1 mm, and not more than 1.1 mm for the maximum (max.) diameters. Error in the areas were lower than 15%, with the exception of VSD
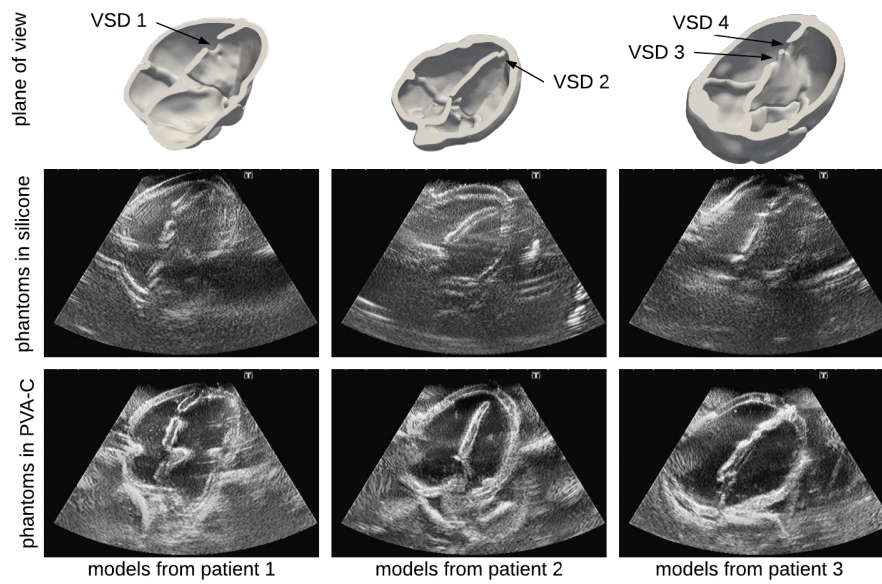
Fig. 7 Visualization of VSDs in ultrasound images acquired from the heart phantoms made of silicone and PVA-C.

3 whose error was 24% (7.4 mm^2). Generally, VSDs in the reconstructed models were smaller than those in the reference ones, with the exception of VSD 4 that was slightly oversized.

Fig. 8 Image of the comparison between reconstructed (red) and reference (green) models for the heart phantoms made of PVA-C.

4 Discussion

We developed a method to build whole heart phantoms of newborns for ultrasound imaging of complex VSDs. We found that ultrasound images acquired from three heart phantoms made of PVA-C showed a better definition of their VSDs than the images acquired from the respective phantoms made of sili-

Table 1 Measurements of areas and diameters (maximum, minimum, mean and standard deviation) of the four ventricular septal defects (VSDs) from the reference (ref.) and reconstructed (rec.) models of the three heart phantoms made of PVA-C.

heart models		VSD	area (mm^2)	diameter (mm)			
				max.	min.	mean	std.
1	ref.	1	44.4	8.8	6.1	7.5	0.9
1	rec.	1	38.1	8.5	5.7	6.9	1.0
2	ref.	2	32.4	8.0	5.0	6.4	1.0
2	rec.	2	32.3	6.9	5.9	6.4	0.3
3	ref.	3	30.9	7.4	4.8	6.2	0.9
3	rec.	3	23.5	6.4	4.4	5.4	0.7
3	ref.	4	31.8	7.0	5.1	6.3	0.6
3	rec.	4	35.1	7.7	5.4	6.6	0.7

Table 2 Error estimation of the measurements of areas and diameters (maximum, minimum, mean and standard deviation) of the four ventricular septal defects (VSDs) from the reference (ref.) and reconstructed (rec.) models of the three heart phantoms made of PVA-C.

heart model	VSD	area error		max. error		min. error		mean error	
		(mm^2)	(%)	(mm)	(%)	(mm)	(%)	(mm)	(%)
1	1	-6.3	-14.2	-0.3	-3.4	-0.4	-6.6	-0.6	-8.0
2	2	-0.1	-0.3	-1.1	-13.8	0.9	18.0	0.0	0.0
3	3	-7.4	-24.0	-1.0	-13.5	-0.4	-8.3	-0.8	-12.9
3	4	3.3	10.4	0.7	10.0	0.3	5.9	0.3	4.8

cone. Image quality from the phantoms made of PVA-C facilitated VSDs size characterization. Results suggest that water-based materials, such as PVA-C, could mimic better tissue echogenicity of cardiac structures than no water-based ones (silicone).

We found good accuracy in sizes of VSDs and shapes of ventricular cavities of the heart phantoms made of PVA-C. However, multiple factors may have contributed to errors in these representations. One of these factors is that each freeze-thaw cycle dehydrated the phantoms making them slightly thinner. Other is the approximations made during acquisition, reconstruction, and segmentation of the ultrasound images. Another factor is that casting and parts assembly involves manual skills. Improvements of these factors, namely fewer freeze-thaw cycles and casting the whole heart as only one piece, could reduce errors, but their implementation is a challenging process.

Our method was designed to build whole heart phantoms as an assembly of two parts. Assembling the parts in silicone was straightforward, but assembling those in PVA-C depended on the material density. Empirically, we found that at least 15% of PVA (by weight) in the hydrogel produces parts rigid enough for successful assembling; lower than that the material consistency hinders the parts merging.

From our experience, we observed that tiny air bubbles attach to the surfaces of the silicone and the PVA-C heart phantoms when they are immersed in water. Removing manually these air bubbles–required for appropriate ultra-

sound imaging–was more difficult from the phantoms in silicone than those in PVA-C. Perhaps this behavior is due to the impermeability and electrostatic properties of the silicone that could keep attached harder the bubbles, which differ from wet materials like PVA-C.

Image segmentation of complex VSDs is very challenging due to the anatomical complexity and limitations in image quality, image resolution, and contrast. Indeed, muscular and membranous fibers interconnected the septum, ventricular walls, and the atrioventricular valves, which misled the definition of VSDs, especially when edges of the defects were misaligned. Therefore, we manually segmented the images under the supervision of a cardiologist. This time-consuming task can take up to 8 hours, which outlines the need for further development of fully automatic segmentation methods [12].

Rapid prototyping methods are evolving very fast and future advances could boost strategies to build phantoms more efficiently. The time to make a full heart phantom with complex VSDs was evaluated between 6 and 10 days: a day for image segmentation; a day for molds design; one to two days for 3-D printing; two and six days for casting in silicone and PVA-C, respectively. This process could be optimized with experience.

We estimated the cost of one heart phantom at $500 USD (in currency of 2021), which includes: $25 materials, $125 renting of machinery, and $350 labor. However, an additional copy of the same heart could cost less than $100 because the molds are reusable. A greater scale production could reduce the materials and machinery costs, but a substantial cost reduction in labor could be achieved by improving the segmentation strategy, namely introducing automatic or semi-automatic segmentation methods to speed up the manual process.

Future work will focus on investigating new approaches to fully automate the segmentation and the identification of VSDs on preoperative imaging, and the incorporation of motion in the phantoms for a more realistic experience [10,13].

5 Conclusion

Rapid prototyping allowed us to formulate and test an approach to build heart phantoms for ultrasound imaging of VSDs. Results suggest that ultrasound images from phantoms made of PVA-C facilitate VSDs size characterization with good accuracy. Future work includes evaluation of the heart phantoms during the simulation of hybrid procedures for closure of complex VSDs.

Declarations

Conflict of interest. The authors declare that they have no conflict of interest.

Ethics approval. Institutional review board approval was obtained for this retrospective study.

Availability of data and material. The clinical datasets cannot be publicly released. The material used in this study is commercially available.

Code availability. Not applicable.

Consent to participate. Not applicable.

Consent for publication. Not applicable.

References

1. Dakkak W, Oliver TI (2020) Ventricular septal defect. StatPearls [Internet]. https://www.ncbi.nlm.nih.gov/books/NBK470330/. Accessed 6 March 2021
2. Amin Z, Berry JM, Foker JE, Rocchini AP, Bass JL (1998) Intraoperative closure of muscular ventricular septal defect in a canine model and application of the technique in a baby. The Journal of thoracic and cardiovascular surgery 115(6):1374–1376. https://doi.org/10.1016/S0022-5223(98)70222-3
3. Harrison CM, Gosai JN (2017) Simulation-based training for cardiology procedures: Are we any further forward in evidencing real-world benefits? Trends in cardiovascular medicine 27(3):163–170. https://doi.org/10.1016/j.tcm.2016.08.009
4. Bhatla P, Tretter JT, Ludomirsky A, Argilla M, Latson LA, Chakravarti S, Barker PC, Yoo SJ, McElhinney DB, Wake N, Mosca RS (2017) Utility and scope of rapid prototyping in patients with complex muscular ventricular septal defects or double-outlet right ventricle: does it alter management decisions? Pediatric cardiology 38(1):103–114. https://doi.org/10.1007/s00246-016-1489-1
5. Morais P, Tavares JMR, Queirós S, Veloso F, D'hooge J, Vilaça JL (2017) Development of a patient-specific atrial phantom model for planning and training of inter-atrial interventions. Medical physics 44(11):5638–5649. https://doi.org/10.1002/mp.12559
6. Laing J, Moore JT, Vassallo R, Bainbridge D, Drangova M, Peters TM (2018) Patient-specific cardiac phantom for clinical training and preprocedure surgical planning. Journal of Medical Imaging 5(2):021222. https://doi.org/10.1117/1.JMI.5.2.021222
7. Alves N, Kim A, Tan J, Hwang G, Javed T, Neagu B, Courtney BK (2020) Cardiac Tissue-Mimicking Ballistic Gel Phantom for Ultrasound Imaging in Clinical and Research Applications. Ultrasound in Medicine & Biology 46(8):2057–2069. https://doi.org/10.1016/j.ultrasmedbio.2020.03.011
8. Wan W, Campbell G, Zhang Z, Hui A, Boughner D (2002) Optimizing the tensile properties of polyvinyl alcohol hydrogel for the construction of a bioprosthetic heart valve stent. Journal of Biomedical Materials Research 63(6):854–861. https://doi.org/10.1002/jbm.10333
9. Surry K, Austin H, Fenster A, Peters T (2004) Poly (vinyl alcohol) cryogel phantoms for use in ultrasound and MR imaging. Physics in Medicine & Biology 49(24):5529. https://doi.org/10.1088/0031-9155/49/24/009
10. Lesniak-Plewinska B, Cygan S, Kaluzynski K, D'hooge J, Zmigrodzki J, Kowalik E, Kordybach M, Kowalski M (2010) A dual-chamber, thick-walled cardiac phantom for use in cardiac motion and deformation imaging by ultrasound. Ultrasound in medicine & biology 36(7):1145–1156. https://doi.org/10.1016/j.ultrasmedbio.2010.04.008
11. Lasso A, Heffter T, Rankin A, Pinter C, Ungi T, Fichtinger G (2014) PLUS: open-source toolkit for ultrasound-guided intervention systems. IEEE transactions on biomedical engineering 61(10):2527–2537. https://doi.org/10.1109/TBME.2014.2322864
12. Decourt C, Duong L (2020) Semi-supervised generative adversarial networks for the segmentation of the left ventricle in pediatric MRI. Computers in Biology & Medicine 123:103884. https://doi.org/10.1016/j.compbiomed.2020.103884
13. Gomes-Fonseca J, Morais P, Queirós S, Veloso F, Pinho AC, Fonseca JC, Correia-Pinto J, Vilaça JL (2018) Personalized dynamic phantom of the right and left ventricles based on patient-specific anatomy for echocardiography studies—Preliminary results. In 2018 IEEE 6th International Conference on Serious Games and Applications for Health (SeGAH). https://doi.org/10.1109/SeGAH.2018.8401362